

A further comparison of solid-state thermionic and thermoelectric refrigeration

T. E. Humphrey^{1,2}, M. F. O'Dwyer³ and A. Shakouri²

¹School of Physics, University of New South Wales, Sydney, N.S.W. 2052, Australia

²Electrical Engineering department, University of California Santa Cruz, Santa Cruz, CA 95060, U.S.A.

³School of Engineering Physics, University of Wollongong, Wollongong, N.S.W. 2522, Australia

Email: tammy.humphrey@unsw.edu.au Web: www.humphrey.id.au

Abstract

We show that the expressions for current and heat current calculated via (the non-linearized) ballistic and diffusive transport formalisms reduce to the same form for solid-state devices one electron mean free path in length. The materials parameters for thermionic and thermoelectric devices are also shown to be equal, rather than differing by a multiplicative constant. We derive a simple transport equation that includes both ballistic and diffusive contributions to the current, and, as an example, use this to calculate the maximum temperature difference obtainable for a piece of Bi₂Te₃ as a function of its length, from less than an electron mean-free path to much greater than a mean-free path. Finally we briefly discuss similarities and differences between thermionic and thermoelectric devices in the regime where device length is of the order of a mean-free path length.

Introduction

It has been shown that thermoelectric and thermionic devices both achieve Carnot efficiency in the same thermodynamic limit; when electron transport between parts of the device that differ in temperature is strictly limited to the energy where the occupation of states is constant [1,2]. Given that the underlying thermodynamics of the two types of devices is the same, it is useful to consider whether there are differences between the devices which become apparent only when non-ideal effects such as phonon heat leaks are taken into account.

A number of previous papers have pointed out similarities in the 'materials parameter' which limits the maximum temperature difference achievable in thermionic and thermoelectric devices [3-5]. Perhaps the most comprehensive comparison was done by Ulrich et al. [5], who found that the materials parameters of thermionic and thermoelectric devices differed by a multiplicative factor of $F_0/F_{1/2}\sqrt{\pi}$, where F_n is a Fermi integral of order n .

Here we point out a minor error in [5] and show that, in fact, the materials parameter of thermionic and thermoelectric devices is identical, and show that the transport formalisms used to describe the two types of devices gives precisely the same results for current, heat current and efficiency for device with a length equal to the electron mean-free path, λ . We further derive a simple expression which considers the contributions of both ballistic and diffusive electron currents for devices with length $L < \lambda$ to $L > \lambda$, and use it to calculate an approximate solution for the maximum temperature difference achievable for Bi₂Te₃ as a function of length. By comparing this to the maximum achievable temperature difference for a device of the same length but with reservoirs which have a lower conduction band edge, we illustrate the

potential advantages of thermionic devices over thermoelectric devices in the ballistic transport regime.

Ballistic and Diffusive transport formalisms for devices with length of the order of an electron mean-free path

Current density in both thermionic and thermoelectric devices can be expressed as

$$J = \iiint j(k)dk \quad (1)$$

where $j(k)\delta k$ is the net 'energy-resolved' current of electrons flowing in the direction opposite to the temperature gradient with momentum in the range δk around k . In thermionic devices with a width less than the mean-free path, most electrons travel ballistically from one reservoir to another. In this case the energy-resolved current density is given by (with dependence upon k implicit)

$$j^b(k)\delta k = qD^r v_x^r \zeta \Delta f \delta k \quad (2)$$

where $D^r(k)$ is the density of states (DOS) in the reservoirs, $\zeta(k)$ is the probability that electrons are transmitted between the reservoirs, $v_x^r(k)$ is the velocity in the direction of transport, given by the dispersion relation $E(k)$ in the reservoirs, and

$$\Delta f = \left[\exp\left(\frac{E(k) - \mu_H}{k_B T_H}\right) + 1 \right]^{-1} - \left[\exp\left(\frac{E(k) - \mu_C}{k_B T_C}\right) + 1 \right]^{-1} \quad (3)$$

is the difference in the Fermi occupation of states in the cold/hot reservoirs and where $\mu_{C/H}$ is the electrochemical potential and $T_{C/H}$ the temperature of electrons at the cold/hot ends of the device.

Here we follow previous work [5] and assume the transmission probability depends upon the total momentum of electrons rather than momentum in the direction of transport only, allowing a direct comparison with thermoelectrics in which the energy of mobile electrons is also restricted in all three dimensions (this assumption is made implicitly in [5] between Eq. 1.1 and Eq. 1.3). The theoretical differences between thermionic devices in which the transmission probability is a function of k and k_x are explored in detail in other papers [6-8].

In thermoelectric devices the energy-resolved diffusive electron current density may be obtained from the Boltzmann transport equation under the relaxation time approximation, and can be written as [9]

$$j^d(k)\delta k = qD^l (v_x^l)^2 \tau(k) \frac{df}{dx} \delta k \quad (4)$$

where $D^l(k)$ is the local DOS, $v_x^l(k)$ is the velocity of electrons in the direction of transport, determined from the local dispersion relation $E(k)$, and $\tau(k) = \tau_0 E(k)^r$ is the relaxation time in the direction of transport.

In solid-state power generators and refrigerators with a width close to the electronic mean-free path it is expected that Eqns (2) and (4) should yield the same results. To show this, we take the energy dependence of the relaxation time to be $r = -1/2$, which corresponds to scattering that is dominated by acoustic phonons and results in a mean-free path in the direction of transport, $\lambda \equiv v_x(k)\tau_0 E^{-1/2}$ which is independent of energy if a dispersion relation of $E(k) = \hbar^2 k^2 / 2m^*$ is assumed. We also note that $df/dx \approx [f(x) - f(x + \delta x)] / \delta x$ when δx is small, so that, for a piece of thermoelectric material L in length, $df/dx \approx \Delta f / L$, and Eqn. (4) becomes

$$j^d(k) \delta k = q \lambda D^l v_x^l \frac{\Delta f}{L} \delta k \quad (5)$$

It can be seen that Eqns. (2) and (5) have an identical form when $L = \lambda$, where the product of $\zeta(k) D^r(k) v_x^r(k)$ in Eq. (2) plays the same role in determining the energy spectrum of electrons which carry current as the product $D^l(k) v_x^l(k)$ does in Eqn. (5). This simple result provides an additional underpinning for Ulrich, Barnes and Vining's observation in [5] that thermionic and thermoelectric devices refrigerate (or generate power) via the same underlying physical mechanism. To show that there is no sharp transition in the behavior of a solid-state power generator or refrigerator as its width changes from $L < \lambda$ to $L > \lambda$, one can use the fact that the probability that an electron can travel a distance L without suffering a collision is [10]

$$P = \exp\left(-\frac{L}{\lambda}\right) \quad (6)$$

to obtain an equation for energy-resolved current density useful in solid-state power generators and refrigerators of length $L \approx \lambda$ as

$$j^d(k) \delta k = \{j^b P + j^d [1 - P]\} \delta k \quad (7)$$

which can easily be generalized to the case where $\lambda \rightarrow \lambda(k)$. We note that Zeng and Chen [11] have addressed in some depth the problem of modeling combined thermionic and thermoelectric effects, including consideration of electron-phonon interaction phenomena, while using Maxwell-Boltzmann statistics to describe thermionic emission boundary conditions at material interfaces, an assumption we avoid in this somewhat simpler analysis.

We can now write down an expression for the net heat current in a solid-state refrigerator of length L as:

$$\begin{aligned} \dot{Q}_C = & \int [E(k) - \mu_C] \{j^b P + j^d [1 - P]\} dk \\ & + \frac{V}{2} \left| \int j^d [1 - P] dk \right| + \frac{\kappa_{ph} \Delta T}{L}. \end{aligned} \quad (8)$$

The first term in Eqn. (8) is negative when there is a net flow of heat carried by electrons from the cold to the hot side of the material. It can be seen that the second last term, accounting for the ohmic heat that returns to the cold side of the device tends to one half in the limit that $L \gg \lambda$, as has previously been pointed out by Shakouri et al. [3]. The last two terms in Eqn. (8) together account for the heat flow back from the hot side of the material via the lattice.

By setting Eqn. (8) to zero, it is possible to calculate the maximum temperature difference, $\Delta T = T_H - T_C$, which can be maintained between the two ends of the device for a particular length of material L . Assuming the dispersion relation $E(k) = \hbar^2 k^2 / 2m^*$, Eqn. (8) can be written as:

$$\begin{aligned} & \int [E - \mu_C] \left\{ \frac{L}{\lambda} \zeta(E + \Delta E) P + E [1 - P] \right\} \Delta f dE \\ & + \frac{qV}{2} \left| \int E [1 - P] \Delta f dE \right| + \frac{\kappa_{ph} \hbar^3}{\lambda 4\pi m^*} \Delta T = 0 \end{aligned} \quad (9)$$

where we have allowed for the fact that the density of states for electrons traveling ballistically can potentially be different to that for electrons which travel diffusively (for example due to a difference in the conduction band offset in the material on either side of the central thermoelectric as indicated in Fig. 1) by introducing an additive factor of ΔE to the ballistic term in the expression.

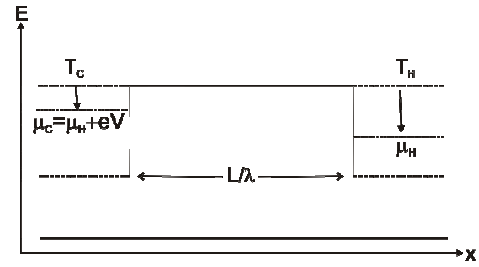


Figure 1: Illustration of the two types of devices considered here. One consists of a single piece of thermoelectric, for example, Bi_2Te_3 . The other can be considered to more closely resemble a thermionic device. It consists of the same piece of thermoelectric sandwiched between two conductors in which the conduction band edge is ΔE meV below the conduction band edge of the central piece of thermoelectric. The primary difference between the two is in the magnitude of DOS for the ballistic component of the current, $D^l(E)$.

It can be seen in Eqn. (8) that the same group of material parameters appear in the last term, irrespective of whether $L \gg \lambda$ such that the system is classified as a thermoelectric, or $L \ll \lambda$, such that the system is classified as a solid-state thermionic device. We have thus shown that these two types of devices share the same materials parameter. It can be shown that the multiplicative constant previously obtained in [5] arose from a discrepancy in assumptions about the energy dependency of the relaxation time [12].

We note that the thermoelectric materials parameter is often expressed in terms of the mobility $\mu_0 = q\tau/m^*$, however in doing this one assumes that the relaxation time is independent of energy, rather than proportional to $E^{-1/2}$ as has been assumed here. In the next section we will look at Bi_2Te_3 as an example in a numerical implementation of Eqn. (9), for which the energy dependence of the relaxation time is usually taken to be $E^{-1/2}$ [13].

Maximum temperature difference for Bi₂Te₃ as a function of material length

To illustrate the smooth transition from predominantly ballistic to predominantly diffusive electron transport as the length of a solid-state refrigerator varies from $L < \lambda$ to $L > \lambda$, we have solved Eqn. (9) for a piece of n-type Bi₂Te₃ material, for which we have taken the following material parameters: $m^* = 0.5m_e$ [13], $\lambda = 500\text{nm}$ [14] and $\kappa_{ph} = 1.5 \text{ Wm}^{-1}\text{K}^{-1}$ [13]. We took the temperature on the hot side of the material to be $T_H = 300\text{K}$ and used a dispersion relation of $E(k) = \hbar^2 k^2 / 2m^*$. We have compared these results with those obtained by using a different density of states for ballistically transmitted electrons. This is intended to simulate in a straightforward way a ‘thermionic’ device, where the conduction band in the reservoirs is generally lower than that of the material forming the ‘barrier’, in this case, Bi₂Te₃.

The numerical procedure was to guess initial values for the energy gap between the conduction band edge and the Fermi energy on the hot side of the material, μ_H (a larger value of μ_H corresponds to a quasi-Fermi energy further away from the band-edge) and the voltage applied between the cold and hot ends of the material, V . We then solve Eqn. (9) for the temperature difference which results in net cooling rate of zero, ΔT . This is the maximum temperature difference obtainable for the initial guesses for μ_H and V . We then varied V to maximize ΔT for the initial guess for μ_H , and then repeated this process for different values of μ_H until we finally obtain the maximum temperature difference, ΔT_{max} for optimized values of μ_H and V .

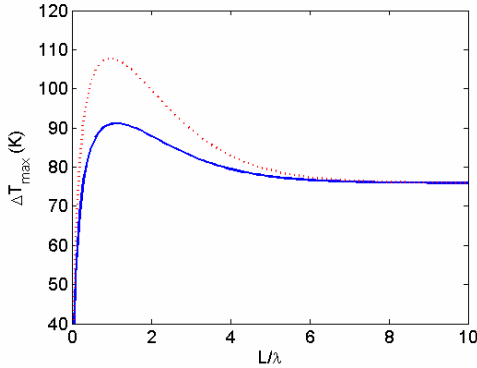


Figure 2: (Blue, solid line) Maximum temperature difference obtainable for Bi₂Te₃ as a function of length normalized on the electron mean free path. (Red, dotted line) Maximum temperature difference for a ‘thermionic’ device, where the density of states for the ballistic component of the current is different from that of the material forming the ‘barrier’.

Results

The results for ΔT_{max} as a function of the length of the material measured in units of the electron mean free path are shown in Fig. 2. The blue solid curve corresponds to the case where the DOS is taken to be the same for both the ballistic and diffusive contributions to the current, and the red, dotted curve to the case where the DOS for the ballistic contribution corresponds to a conduction band edge 30meV below that of

the central piece of Bi₂Te₃ material. Note that the numerically calculated value of ΔT_{max} obtained for $L \gg \lambda$ approaches the experimental value of $\sim 76\text{K}$ for bulk Bi₂Te₃. The values of μ_H and V for which ΔT_{max} was obtained for each value of L/λ are shown in Fig. 3 and 4 respectively, with the electrical current at maximum temperature difference shown in Fig. 5 as a function of L/λ .

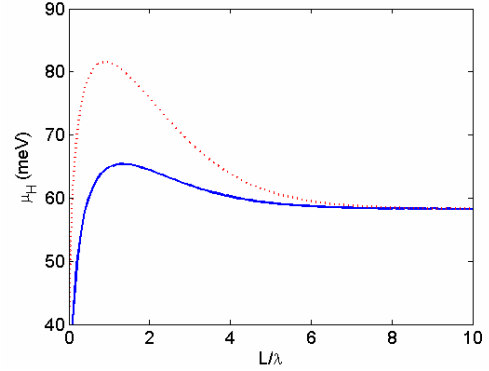


Figure 3: (Blue, solid line) The energy gap between the conduction band and the quasi-Fermi energy on the hot side of the material for which ΔT_{max} is obtained. (Red, dotted line) The energy gap between the conduction band in the ‘barrier’ and the quasi-Fermi energy on the hot side of the material for the ‘thermionic’ device.

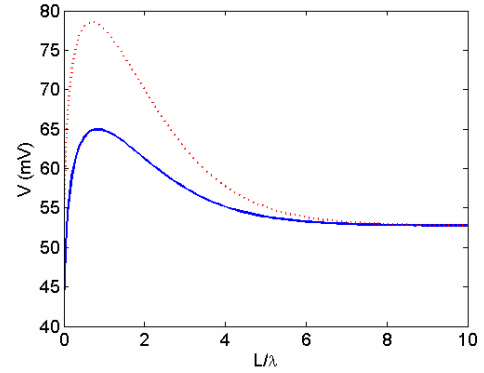


Figure 4: (Blue, solid line) Voltage for which ΔT_{max} is obtained for the ‘thermoelectric’ Bi₂Te₃ device. (Red, dotted line) Voltage for which ΔT_{max} is obtained for the ‘thermionic’ Bi₂Te₃ device.

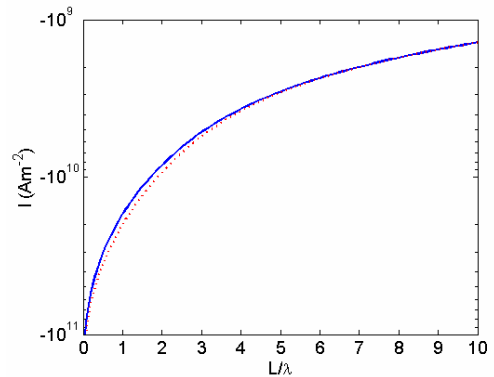


Figure 5: (Blue, solid line) Electrical current for which ΔT_{max} is obtained for the ‘thermoelectric’ Bi₂Te₃ device. (Red, dotted line) Electrical current for which ΔT_{max} is obtained for the ‘thermionic’ Bi₂Te₃ device.

Discussion

Two conclusions can be drawn from Fig. 2. First of all, it can be seen that the maximum temperature difference for Bi_2Te_3 is a function of its length, reaching a maximum at about one electron mean free path ($\sim 500\text{nm}$). However, as the current at this point is around 10^{10} Am^{-2} it would be necessary to have very low contact resistances to take advantage of this effect. The second conclusion that can be drawn from Fig. 2 is that if contact resistances can be made sufficiently small that operating in the ballistic transport regime is useful, the optimum design for a device is a ‘thermionic’ one, where the DOS in the reservoirs is much larger than in the central ‘barrier’ due to the use of a material with a smaller conduction band. The reason why this design gives a substantial increase in ΔT_{max} is that, while the overall magnitude of the current remains approximately the same, as can be seen from Fig. 5 a significantly higher fraction of the current is ballistic, due to the higher DOS in the reservoirs. As the fraction of the current that is ballistic does not produce ohmic heating of the barrier material, the second term in Eqn. (9) becomes smaller. This advantageous effect has been previously pointed out in a number of papers, for example [15,3,6].

It is important to point out that Eqn. (8) remains an approximation to the real situation in a device in which ballistic and diffusive contributions to the electronic current are both significant. An important problem is the accurate determination of the DOS and dispersion relation in such a composite system. Future work will involve the development of a more accurate model to describe solid state refrigerators and generators designed to operate in the regime where $L \approx \lambda$.

Conclusions

We have developed a simple transport equation to describe the regime where device length is on the order of a mean-free path in order to show that the materials parameter which limits the cooling power of a solid-state refrigerator is not dependent upon its length. We have further shown that the usual transport formalisms used to describe thermionic and thermoelectric devices reduce to the same form for device of length equal to the mean free path. Finally, using Bi_2Te_3 as an example, we have calculated the maximum temperature difference obtainable as a function of device length in this material, showing that there is a maximum for devices of length around an electron mean-free path. We have also noted that in this device length regime, an improvement in this maximum temperature difference can be obtained by utilizing a thermionic design which incorporates lower band-gap reservoirs for electrons on either side of the central barrier material.

Acknowledgments

T. H. is supported by the Australian research council and a grant from ONR/MURI.

References

1. Humphrey, T. E., Newbury, R., Taylor, R. P., and Linke, H., “Reversible Quantum Brownian heat engines for electrons”, *Phys. Rev. Lett.*, Vol. 89, (2002), 116801.
2. Humphrey, T. E., and Linke, H., “Reversible thermoelectric nanomaterials”, *Phys. Rev. Lett.*, Vol. 94 (2005), 096601.
3. Shakouri, A. and LaBounty, C. “Materials optimisation for heterostructure integrated thermionic coolers” *Proc. Int. Conf. Thermoelectrics*, Baltimore, MD, Sept. 1999, pp 35-39.
4. Vining, C. B. and Mahan, G. D., “The B factor in multilayer thermionic cooling” *Appl. Phys. Lett.* Vol. 86 (1999), pp 6852-6853.
5. Ulrich, M. D., Barnes, P. A. and Vining, C. B., “Comparison of solid-state thermionic refrigeration with thermoelectric refrigeration”, *J. App. Phys.* Vol. 90 (2001), pp. 1625-1631.
6. Vashaee, D. and Shakouri, A. “Improved thermoelectric power factor in Metal-based superlattices”, *Phys. Rev. Lett.* Vol. 92 (2004) 106103.
7. Humphrey, T. E., O’Dwyer, M. F. and Linke, H. “Power optimization in thermionic devices” *J. Phys. D*, Vol. 38 (2005), pp. 2051-2054.
8. O’Dwyer, M. F., Zhang, C. Lewis, R. and Humphrey, T. E., “Efficiency in nanostructured thermionic and thermoelectric devices” Submitted to *Phys. Rev. B* (2005). Cond-mat/0506388.
9. Kittel, C. Introduction to Solid State Physics, John Wiley & Sons. (New York, 2005).
10. Ashcroft, N. W. and Mermin, N. D., Solid State Physics Saunders College Publishing (Orlando, 1976), p. 249.
11. Zeng, T. and Chen, G. “Interplay between thermoelectric and thermionic effects in heterostructures”, *J. Appl. Phys.* Vol 92, (2002), pp. 3152-3161.
12. Humphrey, T. E., O’Dwyer, M. F., Zhang, C. and Lewis, R. A., “Solid-state thermionics and thermoelectrics in the ballistic transport regime” *J. App. Phys.* (2005). In Press.
13. Nolas, G. S., Sharp, J., Goldsmid, H. J., Thermoelectrics: Basis Principles and New Materials Developments, Springer (Berlin, 2001).
14. Damodara Das, V., and Soundararajan, N., “Size and temperature effects on the thermoelectric power and electrical resistivity of bismuth telluride thin films” *Phys. Rev. B*, Vol. 37 (1988) pp. 4552-4559.
15. Mahan, G. D., Sofo, J. O. and Bartkowiak, M. “Multilayer thermionic refrigerator and generator” *J. Appl. Phys.* Vol 83, (1998) pp. 4683-4689.